Diabatic-state treatment of negative-meson moderation and capture. I. The hydrogen atom

James S. Cohen, Richard L. Martin, and Willard R. Wadt
Theoretical Division, Los Alamos National Laboratory, University of California, Los Alamos, New Mexico 87545
(Received 29 January 1981)

A new formulation of the moderation and capture of negative mesons by atoms has been developed. The scattering is described by a complex potential with a real part given by a diabatic interaction potential and an imaginary part given by the ionization width of the diabatic state embedded in the electronic continuum. Results are presented for collisions of μ^-, π^-, K^-, and p^- with the hydrogen atom. The differential energy-loss cross sections and stopping powers obtained are large. The energy spectrum of stopped mesons is determined and most captures are found to occur at collision energies below or near the ionization potential. The principal-quantum-number distributions of the initially formed mesic atoms peak close to the orbital giving optimal overlap with the displaced electronic orbital. The angular-momentum distributions are not too different from statistical, except that they tend to cut off at l significantly smaller than n-1 in the case of large n. Comparison to a very recent experiment is made in a note added.

I. INTRODUCTION

The capture of negative mesons leading to mesic atom formation has been found experimentally to depend strikingly on the electronic structure of the stopping medium.[1] In this paper we describe a new theoretical formulation for the slowing down and capture of negative mesons at low velocities ($v \lesssim 1$ a.u.$= \alpha c$, the velocity of an electron in the lowest Bohr orbit of the hydrogen atom). Most prior theoretical treatments have been carried out quasiclassically by approximating the stopping medium as an electron gas (e.g., the Fermi-Teller model),[2-5] or quantum mechanically in the Born approximation.[6-11] Although electron-gas models have made impressive progress, they cannot adequately describe few-electron atoms or electronic shell structure, and hence do not provide a realistic basis for understanding the observed chemical dependence. The Born approximation has been applied to capture though not to slowing down. Its validity at low collision velocities is questionable. Recently, Baird[12] has performed a quantum-mechanical perturbed-stationary-state (PSS) calculation for negative-meson–hydrogen-atom collisions using a Born-Oppenheimer description of the meson motion. His calculation is probably the best treatment of negative-meson scattering by the hydrogen atom to date, even though electronically excited bound states were neglected. A much utilized early PSS calculation by Rosenberg[13] is not as reliable because of his use of free-particle continuum wave functions and his assumption of straight-line trajectories. Unfortunately, it would be quite difficult to directly apply the PSS method to other atoms or to molecules. However, Baird's results, which elucidate the role of "adiabatic ionization" for hydrogen,[14-16] suggest a highly physical model which could be more easily applied to many-electron systems.

In the present context, the old qualitative concept of adiabatic ionization simply states that when the meson approaches the hydrogen nucleus closer than the critical dipole distance ($R_c \simeq 0.64 a_0$) the electron becomes free and escapes. The meson energy loss is just the ionization potential plus the unspecified kinetic energy of the free electron. Baird's calculations showed that the electron kinetic energies are almost always low (corresponding to $v_e \lesssim 1$ a.u.). However, he also found that the total ionization cross sections significantly exceed πR_c^2. Moreover, the concept of adiabatic ionization has limited applicability. Consider, for example, the collision of a negative meson with the He atom. As can easily be discerned from the "united-atom" limit, adiabatic ionization does not occur in this case, since H^- is bound. At this point one might well question the efficacy of describing the collision complex in terms of the adiabatic state. If instead one chooses some nonadiabatic, or "diabatic", state, then a potential curve is obtained which may actually cross into the electronic ionization continuum. A nonadiabatic description is further suggested by the fact that the negative meson is accelerated as it approaches the positive nucleus. Of course, if complete sets of states are considered and all potential and nuclear-motion couplings are retained, the two representations are equivalent.[17] One finds, however, that an appropriately chosen nonadiabatic basis can be truncated and that the important couplings assume a more benign form.

Our diabatic state is such that the electronic wave function retains its initial form except possibly for polarization. The state is discrete at all internuclear distances R (Sec. II). At distances where this diabatic state is embedded in the electronic continuum, the transition rate to the continuum, given by the "golden-rule" formula, is evaluated using the Stieltjes moment-theory

technique (Sec. III).[18] Combining this ionization "width" with the real potential energy yields a local complex-potential description of the meson-atom collision in a Born-Oppenheimer framework.[19] The kinetic energy of an electron ejected at a given value of R is distributed about the energy difference between the diabatic and ionic potential curves. Scattering is then calculated quasiclassically (Sec. IV) and the differential energy-loss cross section is determined as a function of initial energy, energy loss, and angular momentum. Very importantly, capture and slowing down are treated on an equal theoretical basis. Using these cross sections we determine the energy spectrum of the stopped mesons as well as the distribution of initial quantum numbers n and l for the newly formed mesic atoms. Results for stopping μ^-, π^-, K^-, and p^- by H atoms are presented in Sec. V and compared with prior calculations in Sec. VI.

II. MESON-ATOM POTENTIAL ENERGY

There are two quite different theoretical points of view for a negative-meson–atom (or molecule) collision: (1) The motion of the meson may be treated self-consistently with the electrons, or (2) the meson may be fixed at a point, as are the nuclei, and the electronic motion in the resulting stationary field calculated. The latter description (Born-Oppenheimer treatment) is adopted in the present work. Within the Born-Oppenheimer framework it is most usual to employ adiabatic states which are eigenstates of the electronic Hamiltonian H_e, neglecting the nuclear and meson kinetic energy terms. The electronic wave function corresponding to the adiabatic description of $H(1s)+\mu^-$ is displayed in Fig. 1 for six $p-\mu^-$ distances. As the negative meson approaches from a large distance, the electronic wave function gradually polarizes toward the opposite side of the nucleus. As the meson comes still closer ($\lesssim 2a_0$) the adiabatic electronic wave function also becomes significantly more diffuse, culminating in a continuum electronic wave function at the distance 0.64 a_0. This calculation was done with an even-tempered Gaussian basis set[20] of 20-s, 20-p, and 20-d functions on hydrogen. The Gaussian exponents are given by $\alpha\beta^n$ where $\alpha=1907$, $\beta=0.4$, and $n=0,1,\ldots,19$. The corresponding adiabatic energies are shown in Fig. 2. The energies obtained with basis functions only on the hydrogen atom agree with the exact values[12] to three decimal places; by adding three s functions and three p functions on the negative meson, another accurate decimal place could be obtained. The energy shown is the electronic energy

$$E_e(R)=\langle\Psi_b(\vec{r},R)|H_e|\Psi_b(\vec{r},R)\rangle, \tag{1}$$

with $\Psi_b=\Psi_b^a$, the adiabatic wave function. The total potential energy is then

$$V(R)=E_e(R)-Z/R, \tag{2}$$

where $Z=1$ for the hydrogen atom.

Within the fixed-meson description it is also possible to define nonadiabatic states which take into account the fact that, in a real collision, the electronic wave function does not really have unlimited time to relax. This effect is well known in atom-atom inelastic scattering[17] and may be especially important for negative muon scattering because of the acceleration of the relatively light meson by the oppositely charged nucleus. The extreme choice of a diabatic state is simply a "frozen-orbital" wave function Ψ_b^d which is not allowed to adjust at all to the presence of the perturbing charge. The potential energy curve resulting from this choice for $H+\mu^-$ is also shown in Fig. 2. This diabatic energy crosses into the continuum at a distance of $R_x=1.86$ a_0. This distance may be compared to $R_c=0.64$ a_0 at which the electron becomes free adiabatically; however, it may be noted that the adiabatic binding energy becomes less than 0.001 a.u. at $R\lesssim 1.0$ a_0.

More accurately, the wave function should show the effect of polarization, which occurs gradually from long-range, but not short-range adiabatic effects which require abrupt changes in the orbital character. In the present work, polarization has been allowed for by introducing a single polarizing configuration. The polarization orbital has been chosen for $H+\mu^-$ in two ways: (1) by considering the perturbation of the isolated H atom by a weak uniform electric field, and (2) by choosing the orbital of p character which minimizes the electronic energy at some finite distance R_p. In the latter case, the result was found to be relatively insensitive to the choice of R_p; a reasonable choice is $R_p=R_x$. This procedure of choosing the polarization orbital is in the spirit of the polarized-orbital method in electron-atom scattering.[21] The results of both procedures are shown in Fig. 2; the two energies differ noticeably only at $R<1$ a_0. At large R the energies with polarization are nearly adiabatic as expected; at smaller R they lie closer to the frozen-orbital diabatic energies.

III. COUPLING TO THE ELECTRONIC CONTINUUM

At distances smaller than the crossing into the continuum, the frozen-orbital diabatic or polarized-orbital diabatic states Ψ_b^d are localized wave functions embedded in the ionization continuum. The ionization width from these discrete states (equal to the transition rate in atomic units) is

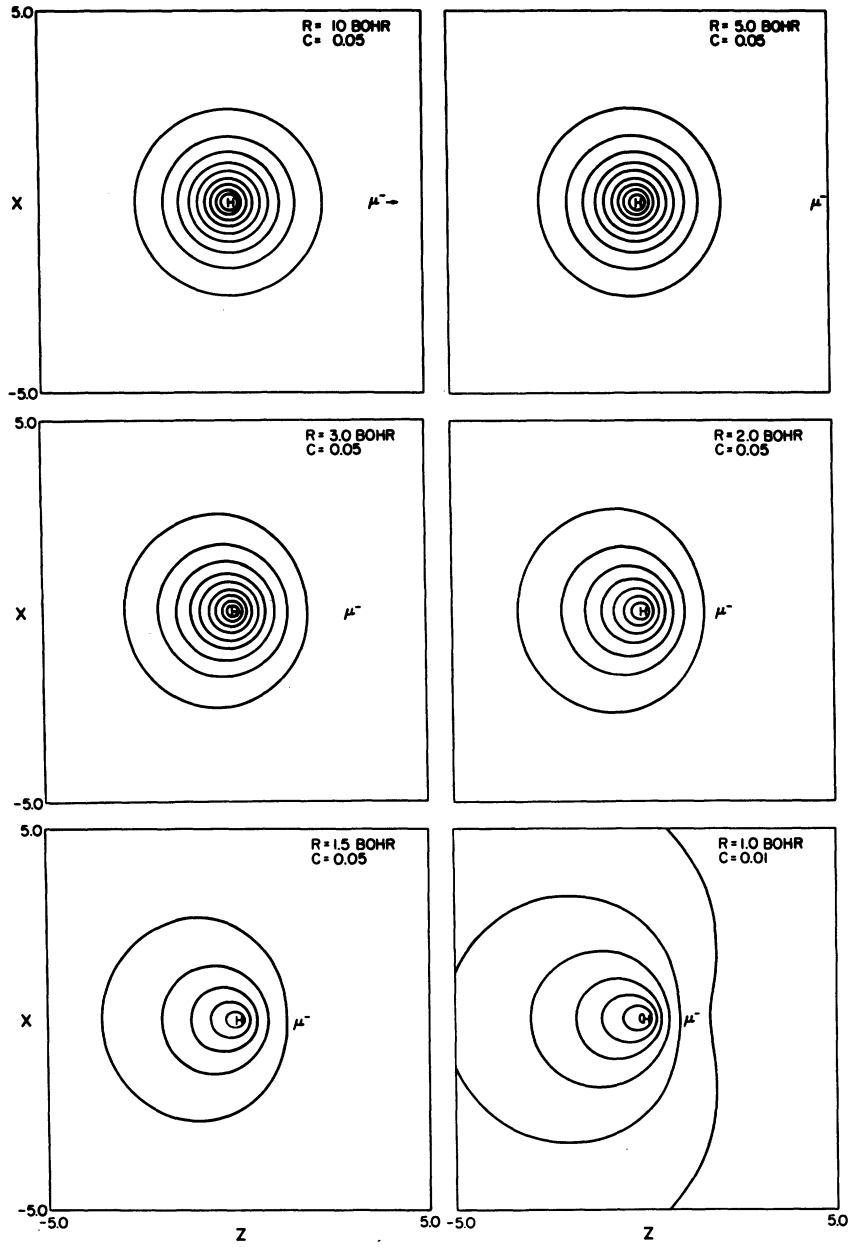

FIG. 1. Contours of the normalized adiabatic electronic wave function for various separations R between the negative meson and hydrogen nucleus. Contour values are C, $2C$, $3C$, ...

given by the golden-rule formula[22]

$$\Gamma(R,\vec{\epsilon}) = 2\pi\rho_\epsilon \left|\langle \mathcal{A}\Psi_c\phi_{\vec{\epsilon}} | H_e - E_b^d | \Psi_b^d \rangle\right|^2 , \qquad (3)$$

where ρ_ϵ is the density of states per unit energy associated with the continuum functions $\phi_{\vec{\epsilon}}$, Ψ_c is the wave function of the system with one electron removed, and $\mathcal{A}$ is the antisymmetrization operator.

The difficulties encountered in evaluating accurate ionization widths are generally not associated with determining accurate bound-state wave functions—quantum chemistry techniques[23] can provide quite good wave functions even for complex polyatomic systems; the problem lies in providing an equally acceptable continuum wave function $\phi_{\vec{\epsilon}}$. To zero-order, $\phi_{\vec{\epsilon}}$ can be approximated by a plane wave, but since Baird's work[12] suggests that most ionization events yield a slow electron, this is not an acceptable approximation. For the specific case of a meson ionizing the hydrogen atom, the exact solution of the Schrödinger equation is possible; i.e., the continuum solution for an electron

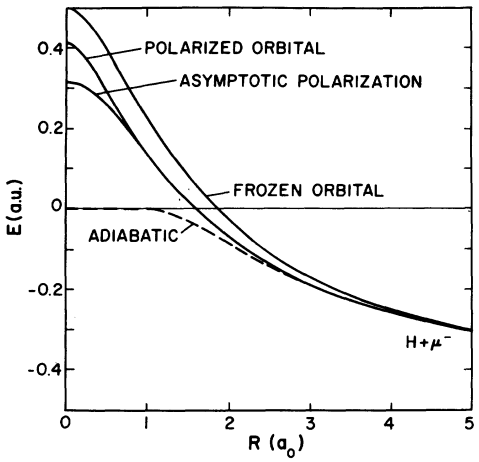

FIG. 2. Electronic potential energy curves for the hydrogen atom plus a negative meson. The meson-nucleus potential has been subtracted out. The dashed curve is the adiabatic energy and the solid curves are three different diabatic approximations.

moving in the field of a dipole is known.[24] Although the exact solution for the next more complicated situation, the motion of a continuum electron in the field of a meson-He^+ core, is not known, recent advances[25] in the theory of electron scattering from diatomic molecules and ions could be applied to generate the static exchange (Hartree-Fock) continuum functions which are of comparable quality to the bound states. These techniques, however, are still incapable of treating even the simplest meson-molecule collision, and so we instead focused on an approach recently suggested by Hazi.[18] This method, which should allow both meson-atom and meson-molecule collisions to be studied, employs a discretization of the continuum coupled with Stieltjes moment theory. It is described in detail elsewhere[18,26] and only the essentials of the theory will be presented here.

Two important concepts form the basis of Hazi's theory. The first is that because the bound-state wave functions which enter into the matrix element (3) fall off exponentially as a function of r, knowledge of the large r behavior of the continuum function is in some sense unnecessary. If affects the magnitude of the matrix element only through a normalization. This suggests an expansion of the continuum in terms of square-integrable functions which have roughly the same spatial extent as the bound states. It is this feature which makes extension of the model to diatomic and polyatomic targets feasible, for the requisite integrals are relatively straightforward to evaluate. In the present work, both the bound states and the continuum are expanded in a basis of Cartesian Gaussian orbitals (CGO) centered on the target atom,

$$\phi_i = N_i x^l y^m z^n e^{-\alpha_i r^2}, \tag{4}$$

where N_i is a normalization factor, and the angular dependence is governed by l, m, and n. For instance, an s-type CGO has $l=m=n=0$, a p_x-type CGO has $l=1$, $m=n=0$, etc.

The linear combination of these CGO's which define the background continuum at each R are found by diagonalizing the electronic Hamiltonian in the space orthogonal to the diabatic state. If a projection operator and its complement are defined,

$$Q = |\Psi_b^d\rangle\langle\Psi_b^d| \tag{5}$$

and

$$P = 1 - Q, \tag{6}$$

then the square-integrable approximations to the continuum functions satisfy

$$\langle\chi_n|PH_eP|\chi_m\rangle = \delta_{nm}\epsilon_n \tag{7}$$

and

$$\langle\chi_n|\chi_m\rangle = \delta_{nm}. \tag{8}$$

The discretized approximation to the width as a function of energy which results from using these square integrable functions directly, i.e.,

$$\gamma_n = 2\pi|\langle\mathcal{A}\chi_n\Psi_c|H_e - E_b^d|\Psi_b^d\rangle|^2, \tag{9}$$

is meaningless because the $\{\chi_n\}$ are improperly normalized. The importance of the set $\{\gamma_n, \epsilon_n\}$ lies in the fact that they can be thought of as providing a set of points and weights which determine the moments of the width distribution. Thus, if the negative moments of $\Gamma(\epsilon)$ are considered

$$S(-k) = \int_{\epsilon_0}^{\infty} \frac{d\epsilon'\Gamma(\epsilon')}{(\epsilon')^k}, \tag{10}$$

it is found that the first few moments are well approximated by

$$S(-k) \simeq \sum_{n=1}^{N} \frac{\gamma_n}{\epsilon_n^k}, \tag{11}$$

as long as $k \ll N/2$.

This fact suggests the second important component of the theory: Given reliable approximations to the first few moments of the distribution, the problem can be inverted to give a (appropriately normalized) histogram approximation to the width distribution. The inversion is justified by Stieltjes moment theory, and the details of the procedure can be found in the papers by Hazi[18] and Langhoff and co-workers.[26]

A practical difficulty with implementing this approach for hydrogen surfaces immediately. When the continuum is imaged with basis sets which include very diffuse functions, the discret-

ization leads to a large number of states whose eigenvalues lie quite close to threshold. Since the ionization threshold in hydrogen occurs at $\epsilon = 0$, this leads to a number of extremely small eigenvalues. In the present work, the smallest eigenvalues are of the order of 10^{-5} a.u. These low-lying states dominate the moments of Eq. (11) and quickly lead to numerical instability in the Stieltjes procedure. This can be avoided by redefining the energy scale; that is, by simply adding a constant to all the eigenvalues before the moment analysis is performed. However, because not all of the moments which can be generated from the set of $\{\gamma_n, \epsilon_n\}$ are used to reconstruct the cumulative width function $F(\epsilon)$, the results can in principle be somewhat affected by the magnitude of the shift. In practice, mutually consistent histogram approximations for $F(\epsilon)$ were obtained from the first 12–20 moments, with shifts in the range 0.1 to 0.5 a.u. When larger numbers of moments were used, wild oscillations arose in the approximation to $F(\epsilon)$, much as is the case in Stieltjes theory applications to photoionization cross sections.[27,28]

The procedure outlined above generates a family of curves $\Gamma(R,\epsilon)$. Conservation of energy dictates that the appropriate function for the optical potential is $\Gamma(R, E_b^d)$, where E_b^d depends parametrically on R, which we denote by simply $\Gamma(R)$. This function for the hydrogen 1s orbital is plotted in Fig. 3. Note that it rises smoothly from a small value near the crossing to a maximum of about 0.58 a.u. at $R = 0$. This behavior is most simply understood in terms of the spatial extent of the diabatic state. Near threshold, the wavelength of the continuum function is too large to overlap appreciably with the H(1s) orbital, but as R decreases and the diabatic state moves higher into the continuum, a better match is found.

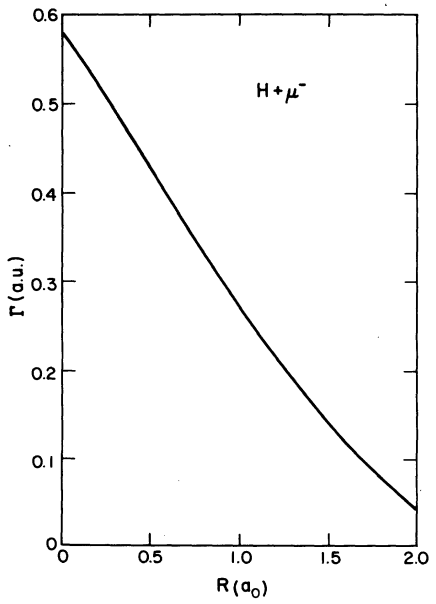

FIG. 3. Ionization width $\Gamma(R)$ for the hydrogen atom plus a negative meson.

IV. ENERGY LOSS IN COLLISIONS

A. Theory

The scattering problem may be formulated in terms of the local complex potential

$$W(R) = V(R) - \frac{i}{2}\Gamma(R), \tag{12}$$

where $V(R)$ and $\Gamma(R)$ have been described in Secs. II and III, respectively (it is assumed that the target is an atom so that the potential depends on R only). The rate of electron emission at distance R between the meson and the atom is given by $\Gamma(R)/\hbar$ ($\hbar = 1$ in atomic units). The meson energy loss when ionization occurs is given by the target ionization potential I_a plus the kinetic energy ϵ carried off by the electron; i.e., the final meson energy is

$$E_f = E - I_a - \epsilon. \tag{13}$$

If $E_f < 0$, the meson is captured; by energy conservation the principal quantum number of the capture orbital is such that $E_n = E_f$, where n is treated as continuous.

For the hydrogen atom

$$n_{\text{capt}} = (-m/2E_f)^{1/2}, \tag{14}$$

where m is the reduced mass of the meson (henceforth, all quantities are in electronic atomic units). Since the meson is typically captured in a rather large orbital, this quasiclassical assignment of n should be adequate. The electron is much lighter than the meson so the l quantum number of the captured meson is about the same as its initial angular momentum, i.e.,

$$l \simeq (2mE)^{1/2} b - \tfrac{1}{2}, \tag{15}$$

where b is the impact parameter.

A useful treatment of the complex-potential scattering problem is the impact-parameter method with quasiclassical trajectories. A given trajectory is specified by its asymptotic velocity v and impact parameter b, or alternatively by its relative energy, $E = \frac{1}{2}mv^2$, and angular momentum l. Letting $p(t)$ be the probability that ionization has occurred by time t, we have the differential equation

$$\frac{dp(t)}{dt} = \Gamma[R(t)][1 - p(t)]. \tag{16}$$

It is more convenient to rewrite the differential equation with R as the independent variable; i.e.,

$$\frac{dp(R)}{dR}=\lambda\left(\frac{m}{2E}\right)^{1/2}\left(1-\frac{b^2}{R^2}-\frac{V(R)}{E}\right)^{-1/2}\Gamma(R)[1-p(R)]. \tag{17}$$

Note that R goes from ∞ to $R_{c1}(\lambda=-1)$, then from R_{c1} to $\infty(\lambda=+1)$, where

$$E-V(R_{c1})-\frac{b^2E}{R_{c1}^2}=0; \tag{18}$$

hence $p(R)$ is double valued and we will denote its two values as $p_{\text{in}}(R)$ and $p_{\text{out}}(R)$. Note that it is not necessary to solve explicitly for the trajectory itself. The total ionization cross section is given by

$$\sigma(E)=2\pi\int_0^\infty p_{\text{out}}(R\to\infty)b\,db. \tag{19}$$

However, results depending on the kinetic energy of the ionized electron are more relevant to slowing down and stopping.

The solution of Eq. (17) gives the probability of ionization as a function of R. At each value of R the electron may have a distribution of kinetic energies ϵ given by a function $f(\epsilon,R)$. To first approximation the electron kinetic energy is just the difference between the diabatic energy $E_b^d(R)$ and ion energy $E_c(R)$, i.e.,

$$f(\epsilon,R)=\delta(\epsilon-\epsilon_0(R)), \tag{20a}$$

where

$$\epsilon_0(R)=E_b^d(R)-E_c(R). \tag{21}$$

When the ionization width is large, as is the case in the present application, the electron energies will be spread out. We approximate this distribution as Lorentzian

$$f(\epsilon,R)=\frac{C(R)}{[\epsilon-\epsilon_0(R)]^2+[\Gamma(R)/2]^2}, \tag{20b}$$

where $C(R)$ is chosen so that

$$\int f(\epsilon,R)d\epsilon=1.$$

The probability of an electron being ejected with energy between ϵ and $\epsilon+d\epsilon$ is then

$$\frac{dP(E,\epsilon,b)}{d\epsilon}d\epsilon=\int_{R_{c1}}^{R_x}f(\epsilon,R)\frac{d}{dR}[-p_{\text{in}}(R)+p_{\text{out}}(R)]\times\left|\frac{d\epsilon_0(R)}{dR}\right|^{-1}dR\,d\epsilon, \tag{22}$$

and the corresponding differential cross section is

$$\frac{d^2\sigma(E,\epsilon,b)}{d\epsilon\,db}=2\pi b\frac{dP(E,\epsilon,b)}{d\epsilon}. \tag{23}$$

The energy-loss cross section is obtained by integrating over the impact parameter,

$$\frac{d\sigma(E,\epsilon)}{d\epsilon}=2\pi\int_0^\infty\frac{dP(E,\epsilon,b)}{d\epsilon}b\,db. \tag{24}$$

From this cross section we get the more easily observed stopping power

$$-\frac{1}{N}\frac{dE}{dx}=\int_0^\infty(I_a+\epsilon)\frac{d\sigma(E,\epsilon)}{d\epsilon}d\epsilon, \tag{25}$$

where N is the target number density.

B. Numerical quadrature

The integrations over electron energy and impact parameter were performed by Gaussian quadrature. First, N_ϵ energy quadrature points ($N_\epsilon\leq 50$) were selected. Separate quadratures were done in the capture and scattering ranges of ϵ. The distances R_i corresponding to these electron energies and the impact parameters b_i having these R values as classical turning points were then determined. Independent N_b-point quadratures ($N_b\leq 4$) over impact parameter were performed between each adjacent pair of b_i. This procedure was designed to avoid the difficulties sometimes associated with numerical integration over classical singularities. The integration of Eq. (17) was carried out using a standard first-order differential equation solver, which was modified to prevent evaluation of the right-hand side of the equation at $R<R_{c1}$.

C. Stopped mesons

It is important to characterize the orbital into which the meson is initially captured since its quantum numbers will determine the subsequent relaxation of the mesic atom via Auger and x-ray emissions. Quasiclassically the quantum numbers are treated as continuous variables. In the case of capture into a bound orbital, i.e., for $I_a+\epsilon>E$, we define

$$\frac{d^2\sigma(E,n,l)}{dn\,dl}=\left|\frac{d\epsilon}{dn}\,\frac{db}{dl}\right|\frac{d^2\sigma(E,\epsilon,b)}{d\epsilon\,db}. \tag{26}$$

For the hydrogen atom we use Eqs. (13)–(15) to get

$$\frac{d^2\sigma(E,n,l)}{dn\,dl}=\frac{1}{n^3v}\frac{d^2\sigma(E,\epsilon,b)}{d\epsilon\,db}. \tag{27}$$

This differential cross section depends on E so before we can determine the distribution of orbitals into which the negative meson is actually captured we must obtain the energy spectrum of the stopped meson. Using the method of Leon[29] we determine the arrival probability density $F_{\text{arr}}(E)$, defined such that the probability of a meson arriving in an energy interval dE is given

by $F_{arr}(E)dE$. The arrival function is determined by the integral equation

$$F_{arr}(E) = \int_0^\infty [1 - P_{capt}(E+\epsilon,\epsilon)] \times\left(\frac{1}{\sigma(E)}\frac{d\sigma(E+\epsilon,\epsilon)}{d\epsilon}\right)F_{arr}(E+\epsilon)\,d\epsilon\,, \quad (28)$$

where $P_{capt}(E,\epsilon)$ is the probability that the meson is captured in a collision at energy E in which an electron of energy ϵ is ejected. If capture at positive energy (i.e., trapping by a centrifugal barrier) can be neglected,[30] then

$$P_{capt}(E,\epsilon) = \Theta(\epsilon + I_a - E)\,,$$

where Θ is the unit step function. We solve for $F_{arr}(E)$ by discretizing Eq. (28), typically using a mesh size of 0.02 a.u. and a constant initial distribution between 14 and 15 a.u. (which integrates to unit probability). For accurate results $\sigma(E)$ must be obtained by a similar quadrature. The capture probability is then given by

$$F_{capt}(E) = F_{arr}(E)\int_0^\infty P_{capt}(E,\epsilon)\left(\frac{1}{\sigma(E)}\frac{d\sigma(E,\epsilon)}{d\epsilon}\right)d\epsilon\,. \quad (29)$$

Hence the probability of the meson being captured in the orbital having quantum numbers n and l is

$$F_{nl} = \int_0^\infty F_{capt}(E)\left(\frac{1}{\sigma(E)}\frac{d^2\sigma(E,n,l)}{dn\,dl}\right)dE\,. \quad (30)$$

V. RESULTS FOR MESONS ON HYDROGEN ATOMS

The total ionization cross sections, given by Eq. (19), are shown in Fig. 4 for collisions of μ^- and p^- with H. The cross sections as a function of velocity are nearly independent of the particular meson mass except at small velocities. As the incident velocity decreases, negative mesons with larger impact parameters are drawn into the ionization region by the nuclear attraction resulting in a very large cross section, especially for the lighter mesons. The ionization probability in Eq. (19) is typically large, e.g., $p_{out}(R\to\infty) \simeq 0.5$ for $v=0.8$ and $b=1.0$. We may note that in the limit that the ionization width is very large a straight-line trajectory calculation would yield an ionization cross section of $\pi R_x^2 = 3.46\,\pi a_0^2$.

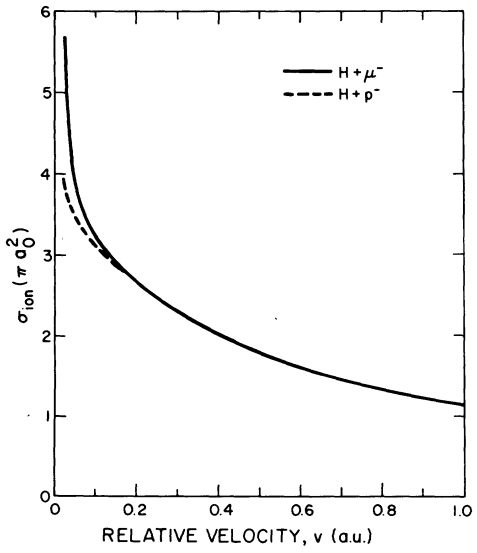

FIG. 4. Total cross sections for ionization of the hydrogen atom by negative mesons.

As mentioned in Sec. IV, the differential energy-loss cross section and related stopping power are more relevant to the stopping of negative mesons. These results depend on the function $f(\epsilon,R)$ which influences the ionized electron kinetic-energy distribution. We present results for both the delta function (20a) and Lorentzian (20b) distributions. The cross section $d\sigma/d\epsilon$, given by Eq. (24), is shown in Fig. 5 for $H+\mu^-$ collisions at three different velocities. The peaks at low electron energies result from ionization occurring near the crossing into the continuum. The distribution of ionization as a function of R is shown in Fig. 6. If a collision is sufficiently slow, then little flux is left at the smaller distances and only low-energy electrons will be ejected; this effect causes the cross section for $v=0.1$ in Fig. 5 to fall below the cross sections for higher velocities in the high electron energy range. The cross sections in Figs. 5(a) and 5(b) are not too different at low electron energies. Of course the maximum electron energy in the delta function case is just the maximum value of $\epsilon_0(R)$ in Eq. (21), which is 0.5 a.u. The Lorentzian

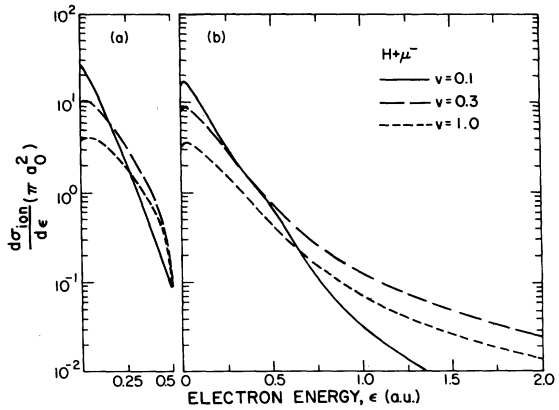

FIG. 5. Energy-differential cross sections for $H+\mu^-$ at three different velocities. Parts (a) and (b) correspond to choices of the delta-function [Eq. (20a)] or Lorentzian [Eq. (20b)] electron-energy distribution, respectively.

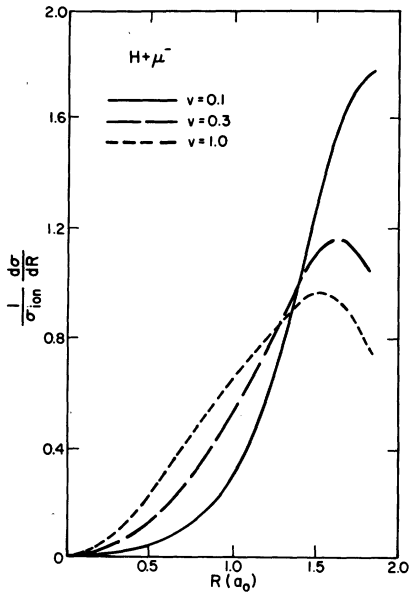

FIG. 6. Profiles of distances at which ionization occurs for $H+\mu^-$ at three different velocities.

distribution has the effect of speading some of the low-energy electrons out to energies greater than 0.5 a.u. At collision velocities above about 0.2 a.u. the energy-loss cross sections for different mesons at the same velocity tend to be about the same, but this is not the case at low velocities from which most captures occur. In regard to capture, it is more instructive to compare the energy loss to the collision energy. In Fig. 7, $d\sigma/d\epsilon$ is compared for the various mesons all undergoing collisions at the same *relative* energy. From this comparison it can be seen

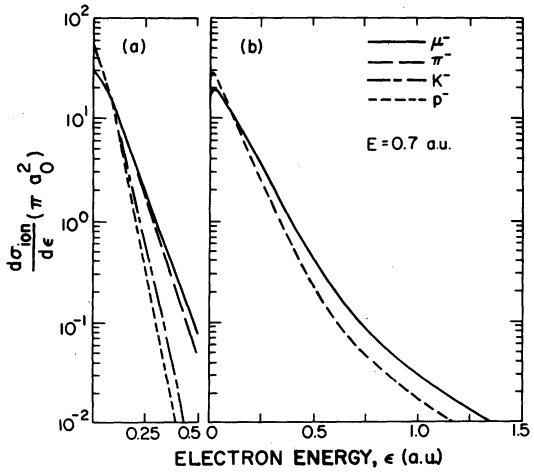

FIG. 7. Energy-differential cross sections at a relative collision energy of 0.7 a.u. Parts (a) and (b) are as in Fig. 5.

that the lighter mesons will be captured into orbitals lying at somewhat lower energies.

From the energy-loss cross section it is a simple matter to calculate the stopping power [see Eq. (25)]. The stopping powers are plotted in Fig. 8. The use of the Lorentzian spread of electron energies increases the calculated stopping power by about 25%.

The stopped mesons can be characterized as discussed in Sec. IV C. The relative energies of the mesons (in the center-of-mass system) just before capture are plotted in Fig. 9. Note that each curve must integrate to unit probability. The effect of the Lorentzian spread of electron energies is that about 8% of the mesons get captured in higher energy collisions than in the delta-function case. The slope is not really discontinuous at 0.5 a.u. and the curve there would be smoother if inelastic (nonionizing) processes were included. Since we assume all energy loss occurs via ionization, the capture probability is the same as the arrival probability at energies below 0.5 a.u. The arrival probability is a fairly flat function of energy[31]; hence a "white" spectrum would not be a bad approximation in this case.[29,32]

The probabilities of capture into an orbital with given quantum numbers are shown in Figs. 10 and 11. In Fig. 10 the probabilities are summed over l. The n distribution peaks close to the value which has maximum radial density at the same distance as the normal hydrogen atom, i.e.,

$$n_{\max} \simeq \sqrt{m}$$

($m = 185.9$ for μ^-, 237.8 for π^-, 633.2 for K^-, and 918.1 for p^-). The most important effect of the Lorentzian spread of electron kinetic energies is capture into lower-lying principal quantum numbers; nevertheless, the results clearly predict that the probability of capture rapidly decreases as n falls below $n_{\max}$. At $n > n_{\max}$, F_n behaves nearly as n^{-3}, corresponding to an ap-

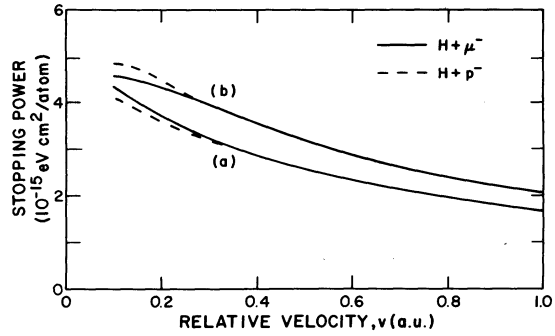

FIG. 8. Stopping powers (per atom) for negative mesons by hydrogen atoms. Curves (a) and (b) are as in Fig. 5.

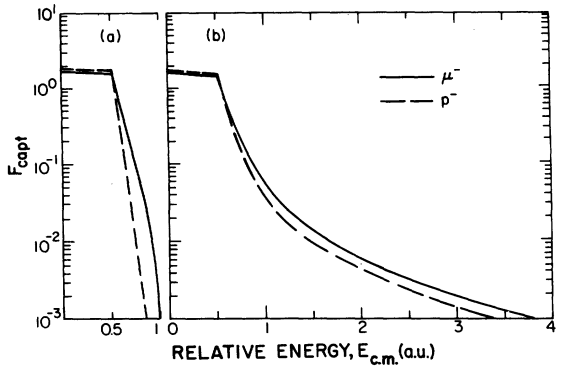

FIG. 9. Spectra of meson energies just prior to capture. Parts (a) and (b) are as in Fig. 5.

proximately uniform distribution in binding energy,[32] from zero to I_a. The l distributions, shown in Fig. 11 for selected values of n, are particularly important as input to cascade calculations. The populations start out statistical at small l (i.e., proportional to $2l+1$), increase somewhat more rapidly at intermediate l and in some cases decrease abruptly at a value of l smaller than the largest permissible value. The cut off is more pronounced for the lighter mesons and for the larger n values. In Table I the average l values are given and compared with the values corresponding to a statistical distribution.

VI. DISCUSSION

We can summarize our principal conclusions about moderation and capture of negative mesons by hydrogen atoms as follows.

(1) The total ionization cross section is large ($\sim \pi R_x^2$) and has a fairly weak dependence on incident energy.

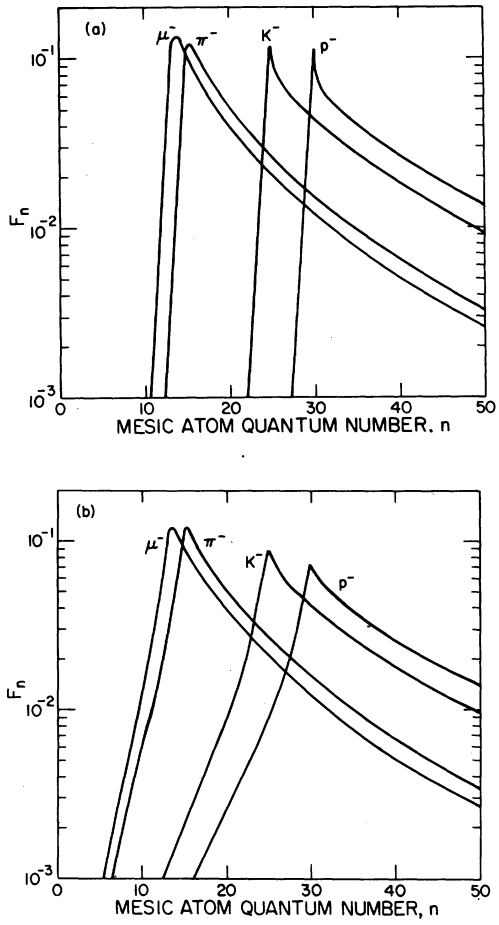

FIG. 10. Spectra of n values for initially captured negative mesons. Parts (a) and (b) are as in Fig. 5.

TABLE I. Average angular momentum in orbital of initial capture for the delta-function distribution (a) and Lorentzian distribution (b) of electron kinetic energies. The result for a statistical population (c) is given for comparison.

	n = 5	10	15	20	30	40	50
				(a)			
$\bar{l}(\mu^-)$		3.5	9.1	13.5	16.0	16.2	16.6
$\bar{l}(\pi^-)$			6.5	13.4	17.1	17.7	18.8
$\bar{l}(K^-)$				6.5	19.0	25.3	28.1
$\bar{l}(p^-)$					11.8	27.6	32.0
				(b)			
$\bar{l}(\mu^-)$	2.8	5.8	9.4	13.2	16.5	17.4	17.8
$\bar{l}(\pi^-)$	2.8	6.0	7.9	13.1	17.9	19.4	20.0
$\bar{l}(K^-)$		6.1	9.4	12.0	19.7	26.3	29.8
$\bar{l}(p^-)$		6.1	9.5	12.6	15.5	26.7	32.8
				(c)			
$\bar{l}_{stat}$	2.8	6.2	9.5	12.8	19.5	26.2	32.8

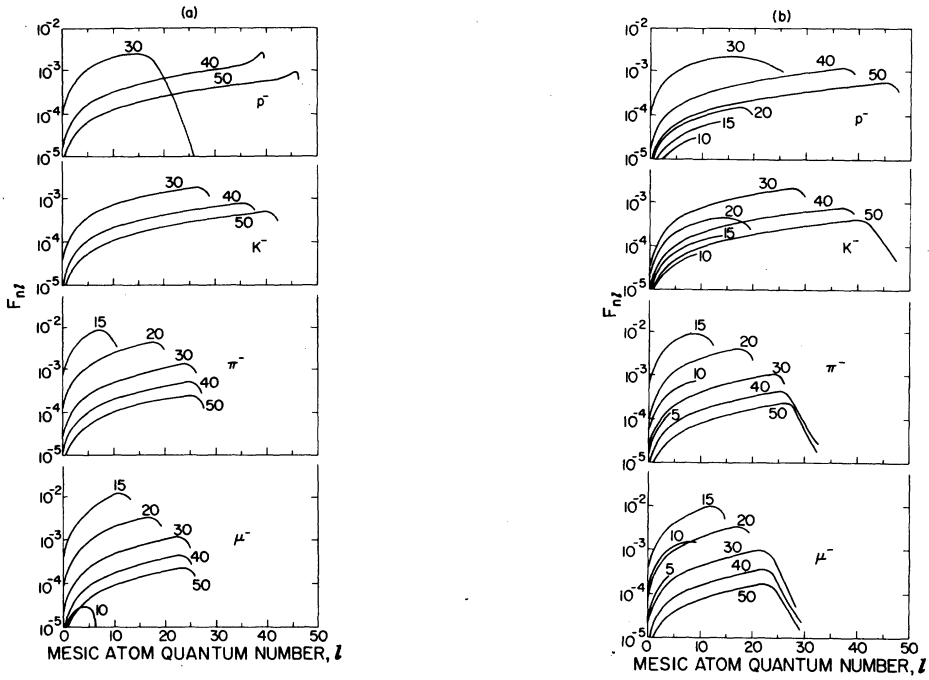

FIG. 11. Spectra of l values for negative mesons initially captured in orbitals having the designated n values. Parts (a) and (b) are as in Fig. 5.

(2) The main energy loss is due to the target's ionization potential.

(3) Most mesons are stopped at low energies ($\lesssim 30$ eV).

(4) The most probable capture orbital has large overlap with the displaced electronic orbital ($n_{max} \simeq \sqrt{m}$).

(5) The angular-momentum distributions for the captured meson are not too far from statistical but tend to cut off at large values in the case of large n and light mesons.

Our total ionization cross section is somewhat smaller than that obtained by Baird[12] in a two-state PSS calculation but is still appreciably larger than that predicted by the adiabatic ionization model. We agree with Baird that the kinetic energies of the ejected electrons tend to be low and consequently most mesons are slowed to low energies before being captured. Capture at low energies, which is also predicted from Baird's energy-loss cross section,[12,32] is in disagreement with the Born-approximation papers which predict capture mostly at energies exceeding 50 eV. It is not clear, however, whether this discrepancy reflects disagreement with the Born approximation itself or with the method used to obtain the stopped meson spectrum. The ambiguity arises from the fact that only the capture cross sections but not the equally relevant slowing down cross sections were calculated in the Born approximation. The energy at which the mesons are stopped depends on the competition between these two processes which we calculate in parallel. In this regard we note that our stopping power slows mesons from $v=1.0$ a.u. to $v=0.1$ a.u., about 6 times as fast as does the stopping power of Rosenberg[13] which was assumed by Haff and Tombrello[10] and by Korenman and Rogovaya.[11]

Note added. Shortly after this paper was submitted we learned of the first experimental determination of the moderation time for negative muons in hydrogen gas. Anderhub *et al.*[33] at SIN found that a 2-keV muon in 1-Torr hydrogen was captured in 170 ± 40 ns and that this stopping time scaled inversely with pressure. Our theoretical prediction, using the stopping power (b) in Fig. 8, is 180 ns. The theory is for H atoms while the experiment is done with H_2, but the agreement is nevertheless quite satisfactory.

ACKNOWLEDGMENTS

We are grateful to Dr. Mel Leon and Dr. David Cartwright for suggesting this problem. We thank them and Dr. Andrew Hazi for helpful discussions. This work was supported in part by the New Research Initiatives Program of Los Alamos Scientific Laboratory and was performed under the auspices of the U.S. Department of Energy.

[1]L. I. Ponomarev, Ann. Rev. Nucl. Sci. 23, 395 (1973); S. S. Gershtein and L. I. Ponomarev, in *Muon Physics*, edited by V. W. Hughes and C. S. Wu (Academic, New York, 1975), Vol. III, p. 141.
[2]E. Fermi and E. Teller, Phys. Rev. 72, 399 (1947).
[3]M. Leon and R. Seki, Phys. Rev. Lett. 32, 132 (1974); Nucl. Phys. A282, 445 (1977); M. Leon and J. H. Miller, *ibid.* A282, 461 (1977).
[4]P. K. Haff, P. Vogel, and A. Winther, Phys. Rev. A 10, 1430 (1974); P. Vogel, P. K. Haff, V. Akylas, and A. Winther, Nucl. Phys. A 254, 445 (1975).
[5]H. Daniel, Phys. Rev. Lett. 35, 1649 (1975).
[6]A. H. deBorde, Proc. Phys. Soc. (London) 67A, 57 (1954).
[7]G. A. Baker, Phys. Rev. 117, 1130 (1960).
[8]R. A. Mann and M. E. Rose, Phys. Rev. 121, 293 (1961).
[9]A. D. Martin, Nuovo Cimento 27, 1359 (1963).
[10]P. K. Haff and T. A. Tombrello, Ann. Phys. (N. Y.) 86, 178 (1974).
[11]G. Ya. Korenman and S. I. Rogovaya, Yad. Fiz. 22, 754 (1975) [Sov. J. Nucl. Phys. 22, 389 (1976)]; J. Phys. B 13, 641 (1980).
[12]T. J. Baird, Ph.D. thesis, Rensselaer Polytechnic Institute, 1976 (unpublished) and Los Alamos Report LA-6619-T.
[13]R. L. Rosenberg, Philos. Mag. 40, 759 (1949).
[14]A. S. Wightman, Phys. Rev. 77, 521 (1950).
[15]S. S. Gershtein, Zh. Eksp. Teor. Fiz. 39, 1170 (1960) [Sov. Phys.—JETP 12, 815 (1961)].
[16]H. S. W. Massey, E. H. S. Burhop, and H. B. Gilbody, *Electronic and Ionic Impact Phenomena: Slow Positron and Muon Collisions*, 2nd ed. (Clarendon, Oxford, 1974), Vol. V, Chap. 27.
[17]F. T. Smith, Phys. Rev. 179, 111 (1969).
[18]A. U. Hazi, J. Phys. B 11, L259 (1978).
[19]T. F. O'Malley, Phys. Rev. 150, 14 (1966).
[20]R. C. Raffenetti, J. Chem. Phys. 59, 5936 (1973).
[21]A. Temkin and J. C. Lamkin, Phys. Rev. 121, 788 (1961).
[22]W. H. Miller, Chem. Phys. Lett. 4, 627 (1970).
[23]*Modern Theoretical Chemistry*, Vols. III and IV, edited by H. F. Schaefer (Plenum, New York, 1977).
[24]See, e.g., L. I. Ponomarev and L. N. Somov, J. Comput. Phys. 20, 183 (1976).
[25]*Electron-Molecule and Photon-Molecule Collisions*, edited by T. Rescigno, V. McKoy, and B. Schneider (Plenum, New York, 1979).
[26]P. W. Langhoff, C. T. Corcoran, J. S. Sims, F. Weinhold, and R. M. Glover, Phys. Rev. A 14, 1042 (1976).
[27]R. L. Martin, W. R. Daasch, and E. R. Davidson, J. Chem. Phys. 71, 2375 (1979).
[28]See the article by P. W. Langhoff in Ref. 25.
[29]M. Leon, Phys. Rev. A 17, 2112 (1978).
[30]Capture at positive energies does not occur with hydrogen atom targets, but may be important for many-electron targets. See, e.g., Ref. 29.
[31]For example, $F^{(a)}_{arr}(0)=1.07\,F^{(a)}_{arr}(4)$ and $F^{(b)}_{arr}(0)=1.27\,F^{(b)}_{arr}(4)$ for $H+\mu^-$.
[32]M. Leon, in *Exotic Atoms '79*, edited by K. Crowe, J. Duclos, G. Fiorentini, and G. Torelli (Plenum, New York, 1980), p. 141.
[33]H. Anderhub, J. Böcklin, M. Devereux, F. Dittus, R. Ferreira Marques, H. Hofer, H. K. Hofer, F. Kottmann, O. Pitzurra, P.-G. Seiler, D. Taqqu, J. Unternährer, M. Wälchli, and Ch. Tschalär, Phys. Lett. B (in press).